PROCEEDINGS OF SCIENCE

Transverse momentum distribution of charged particles and identified hadrons in p–Pb collisions at the LHC with ALICE

Roberto Preghenella* **for the ALICE Collaboration**
Centro Studi e Ricerche e Museo Storico della Fisica "Enrico Fermi", Rome, Italy
Sezione INFN, Bologna, Italy
E-mail: roberto.preghenella@bo.infn.it

Hadron production has been measured at mid-rapidity by the ALICE experiment at the LHC in proton-lead (p–Pb) collisions at $\sqrt{s_{\rm NN}}$ = 5.02 TeV. The transverse momentum ($p_{\rm T}$) distribution of primary charged particles and of identified light-flavoured hadrons ($\pi^{\pm}$, $\rm K^{\pm}$, $\rm K^0_S$, p, $\bar{\rm p}$, Λ, $\bar{\Lambda}$) are presented in this report. Charged-particle tracks are reconstructed in the central barrel over a wide momentum range. Furthermore they can be identified by exploiting specific energy loss (dE/dx), time-of-flight and topological particle-identification techniques. Particle-production yields, spectral shapes and particle ratios are measured in several multiplicity classes and are compared with results obtained in Pb–Pb collisions at the LHC.

The measurement of charged-particle transverse momentum spectra and nuclear modification factor $\rm R_{pPb}$ indicates that the strong suppression of high-$p_{\rm T}$ hadrons observed in Pb–Pb collisions is not due to initial-state effects, but it is rather a fingerprint of jet quenching in hot QCD matter. The systematic study of the hadronic spectral shapes as a function of the particle mass and of particle ratios as a function of charged-particle density provides insights into collective phenomena, as observed in Pb–Pb collisions. Similar features, that could be present in high-multiplicity p–Pb collisions, will also be discussed.

The European Physical Society Conference on High Energy Physics – EPS-HEP2013
18-24 July 2013
Stockholm, Sweden

*Speaker.

PoS(EPS-HEP 2013)188

1. Introduction

High-energy heavy-ion (AA) collisions offer a unique possibility to study hadronic matter under extreme conditions, in particular the deconfined quark-gluon plasma which has been predicted by quantum chromodynamics (QCD) [1–4]. The interpretation of the results depends crucially on the comparison with results from smaller collision systems such as proton-proton (pp) or proton-nucleus (pA). Proton-nucleus (pA) collisions are intermediate between proton-proton (pp) and nucleus-nucleus (AA) collisions both in terms of system size and number of produced particles. Comparing particle production in pp, pA, and AA reactions is frequently used to separate initial state effects, connected to the use of nuclear beams or targets, from final state effects, connected to the presence of hot and dense matter. Moreover, pA collisions allow for the investigation of fundamental properties of QCD; the p_{T} distributions and yields of particles of different mass at low and intermediate momenta of $p_{\mathrm{T}} \lesssim 3$ GeV/c (where the vast majority of particles is produced) can provide important information about the system created in high-energy hadron reactions.

Previous results on identified particle production in pp and Pb–Pb collisions at the LHC have been reported in [5–11]. Results on transverse momentum distribution and nuclear modification factor of charged particles in p–Pb collisions at $\sqrt{s_{\mathrm{NN}}}$ = 5.02 TeV have been reported in [12]. In this paper we report on the measurement of $\pi^{\pm}$, $\mathrm{K}^{\pm}$, K^0_S, $\mathrm{p}(\overline{\mathrm{p}})$ and $\Lambda(\bar{\Lambda})$ production in p–Pb collisions at a nucleon-nucleon center-of-mass energy $\sqrt{s_{\mathrm{NN}}}$ = 5.02 TeV.

2. Sample and Data analysis

The results presented here were obtained from a sample of the data collected during the LHC p–Pb run at $\sqrt{s_{\mathrm{NN}}}$ = 5.02 TeV in the beginning of 2013. Due to the asymmetric beam energies for the proton and lead beams, the nucleon-nucleon center-of-mass system was moving in the laboratory frame with a rapidity of $y_{\mathrm{NN}} = -0.465$ in the direction of the proton beam. A detailed description of the ALICE apparatus can be found in [13] and a description of the data-taking and trigger setup in minimum-bias trigger in [14]. In order to study the multiplicity dependence, the selected event sample was divided into seven event classes, based on cuts applied on the total charge deposited in the VZERO-A scintillator hodoscope ($2.8 < \eta_{\mathrm{lab}} < 5.1$, Pb beam direction).

The ALICE central-barrel tracking covers the full azimuth within $|\eta_{\mathrm{lab}}| < 0.9$. The tracking detectors are located inside a solenoidal magnet providing a magnetic field of 0.5 T. The innermost barrel detector is the Inner Tracking System (ITS). The Time Projection Chamber (TPC), the main central-barrel tracking device, follows outwards. Finally the Transition Radiation Detector (TRD) extends the tracking farther away from the beam axis. Charged-hadron identification in the central barrel was performed with the ITS, TPC [15] and Time-Of-Flight (TOF) [16] detectors [17]. Three approaches were used for the identification of $\pi^{\pm}$, $\mathrm{K}^{\pm}$, and $\mathrm{p}(\bar{\mathrm{p}})$, called "ITS standalone", "TPC/TOF" and "TOF fits" and are described in details in [8, 9]. Contamination from secondary particles was subtracted with a data-driven approach, based on the fit to the transverse distance-of-closest approach to the primary vertex (DCA_{xy}) distribution with the expected shapes for primary and secondary particles [8, 9].

The K^0_S and $\Lambda(\bar{\Lambda})$ particles were identified exploiting their "V^0" weak decay topology in the channels $\mathrm{K}^0_S \to \pi^+\pi^-$ and $\Lambda(\bar{\Lambda}) \to \mathrm{p}\pi^-(\bar{\mathrm{p}}\pi^+)$. The selection criteria used to define two tracks as

V^0 decay candidates are detailed in [6, 18]. The contribution from weak decays of the charged and neutral Ξ to the $\Lambda(\bar{\Lambda})$ yield has been corrected following a data-driven approach.

The study of systematic uncertainties follows the analysis described in [6, 8, 9, 18] and was repeated for the different multiplicity bins in order to separate the sources of uncertainty which are dependent on multiplicity and uncorrelated across different bins (depicted as shaded boxes in the figures).

3. Results

The p_{T} distributions of $\pi^{\pm}$, $\mathrm{K}^{\pm}$, K^0_S, $\mathrm{p}(\overline{\mathrm{p}})$ and $\Lambda(\bar{\Lambda})$ in $0 < y_{\mathrm{CMS}} < 0.5$ are reported in [19] for different multiplicity intervals. Particle/antiparticle as well as charged/neutral kaon transverse momentum distributions are identical within systematic uncertainties. The p_{T} distributions show a clear evolution, becoming harder as the multiplicity increases. The multiplicity dependence of the p_{T} spectral shape is stronger for heavier particles, as evident when looking at the ratios $\mathrm{K}/\pi = (\mathrm{K}^+ + \mathrm{K}^-)/(\pi^+ + \pi^-)$, $\mathrm{p}/\pi = (\mathrm{p} + \overline{\mathrm{p}})/(\pi^+ + \pi^-)$ and Λ/K^0_S as functions of p_{T}, shown in Fig. 1 for the 0–5% and 60–80% event classes. The ratios p/π and Λ/K^0_S show a significant enhancement at intermediate $p_{\mathrm{T}} \sim 3$ GeV/c, qualitatively reminiscent of the one measured in Pb–Pb collisions [8, 9, 18]. The latter is generally discussed in terms of collective flow or quark recombination [20–22]. A similar enhancement of the p/π ratio in high-multiplicity d–Au collisions has also been reported for RHIC energies [23].

It is worth noticing that the ratio p/π as a function of $\mathrm{d}N_{\mathrm{ch}}/\mathrm{d}\eta$ in a given p_{T}-bin follows a power-law behavior: $\frac{\mathrm{p}}{\pi}(p_{\mathrm{T}}) = A(p_{\mathrm{T}}) \times [\mathrm{d}N_{\mathrm{ch}}/\mathrm{d}\eta]^{B(p_{\mathrm{T}})}$. As shown in Fig. 2, the same trend is also observed in Pb–Pb collisions. The exponent of the power-law function exhibits the same value in both collision systems (Fig. 3, left). The same feature is also observed in the Λ/K^0_S ratio and this also holds in pp collisions (Fig. 3, right).

4. Discussion

In heavy-ion collisions, the flattening of transverse momentum distribution and its mass ordering find their natural explanation in the collective radial expansion of the system [24]. This picture can be tested in a blast-wave model [25] with a simultaneous fit to all particles. This parameterization assumes a locally thermalized medium, expanding collectively with a common velocity field and undergoing an instantaneous common freeze-out. The fit presented here is performed in the same range as in [8, 9], also including K^0_S and $\Lambda(\bar{\Lambda})$. The results are reported Fig. 4. Variations of the fit range lead to large shifts ($\sim 10\%$) of the fit results (correlated across centralities), as discussed for Pb–Pb data in [8, 9]. As can be seen in Fig. 4, the parameters show a similar dependency with event multiplicity as observed with the Pb–Pb data. Within the limitations of the blast-wave model, this observation is consistent with the presence of radial flow in p–Pb collisions. Under the assumptions of a collective hydrodynamic expansion, a larger radial velocity in p–Pb collisions has been suggested as a consequence of stronger radial gradients in [26]. On the other hand it is worth noticing that very similar results are obtained when performing the same study on pp spectra measured as a function of the event multiplicity. Other processes not related to hydrodynamic collectivity could also be responsible for the observed results. This is illustrated

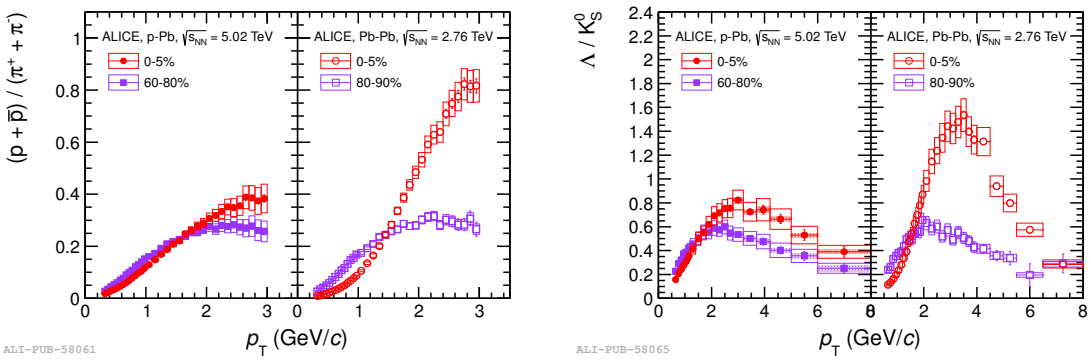

Figure 1: Ratios p/π (left) and Λ/K^0_S (right) as a function of p_T in two multiplicity bins compared to results in Pb–Pb collisions. The empty boxes show the total systematic uncertainty; the shaded boxes indicate the contribution uncorrelated across multiplicity bins (not estimated in Pb–Pb).

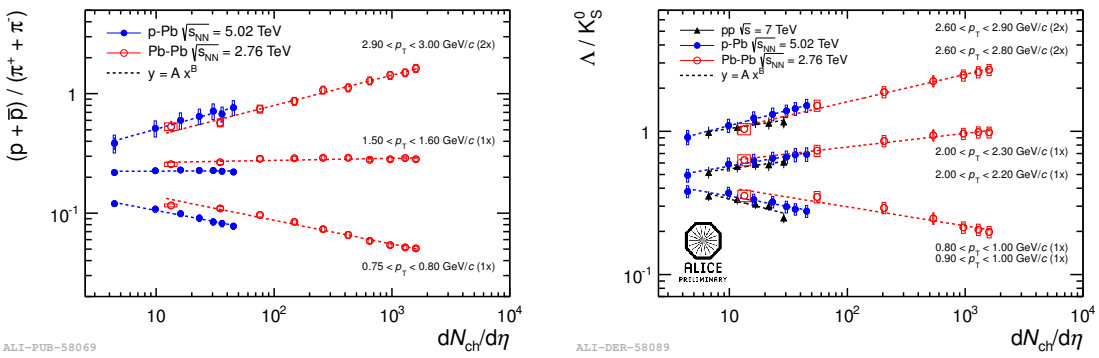

Figure 2: Ratios p/π (left) and Λ/K^0_S (right) as a function of the charged-particle density $dN_{ch}/d\eta$ in three p_T intervals in p–Pb, Pb–Pb and pp collisions (pp only shown for Λ/K^0_S). The dashed lines show the corresponding power-law fit.

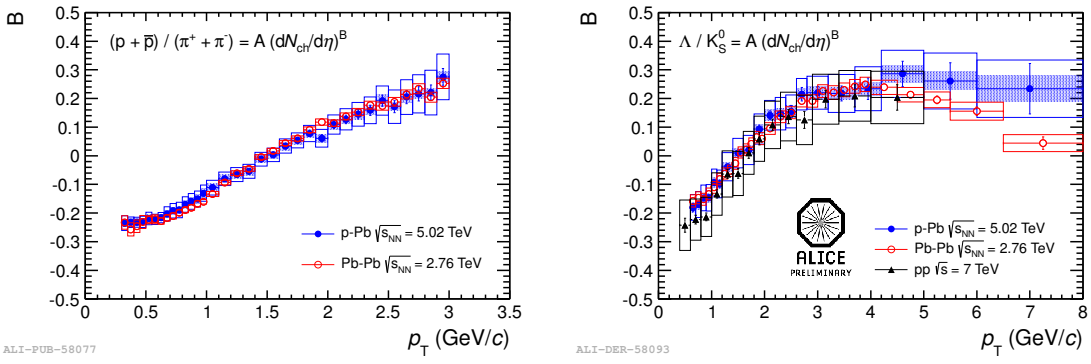

Figure 3: Exponent of the p/π (left) and Λ/K^0_S (right) power-law fit as a function of p_T in p–Pb, Pb–Pb and pp collisions (pp only shown for Λ/K^0_S).

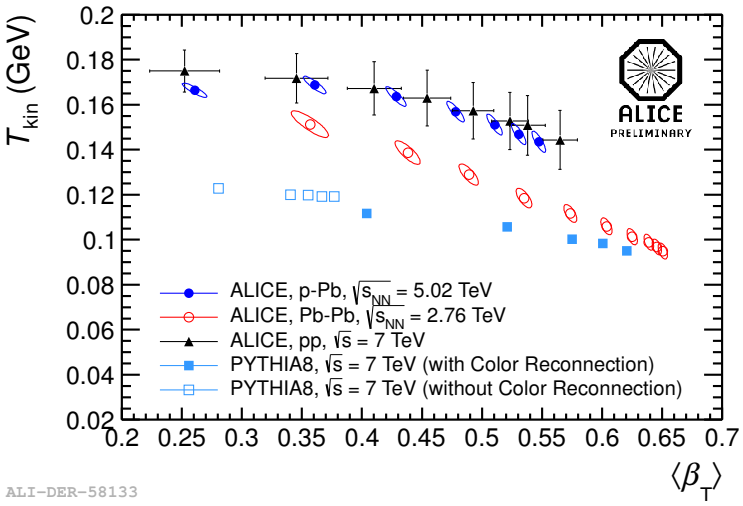

Figure 4: Results of blast-wave fits, compared to Pb–Pb data, pp data and MC simulations from PYTHIA8 with and without color reconnection. Charged-particle multiplicity increases from left to right. Uncertainties from the global fit are shown as correlation ellipses for p–Pb and Pb–Pb data and with errors bars for pp data.

in Fig. 4, which shows the results obtained by applying the same fitting procedure to transverse momentum distributions from the simulation of pp collisions at $\sqrt{s}$ = 7 TeV with the PYTHIA8 event generator (tune 4C) [27], a model not including any collective system expansion. The fit results are shown for PYTHIA8 simulations performed both with and without the color reconnection mechanism [28, 29]. With color reconnection the evolution of PYTHIA8 transverse momentum distributions follows a similar trend as the one observed for p–Pb, pp and Pb–Pb collisions at the LHC, while without color reconnection it is not as strong. This generator study shows that other final state mechanisms, such as color reconnection, can mimic the effects of radial flow [30].

The p_{T} distributions in the 5-10% bin are compared in Fig. 5 with calculations from the DPMJET [31], Kraków [32] and EPOS LHC 1.99 v3400 [33] models. The transverse momentum distributions in the 5-10% multiplicity class are compared to the predictions by Kraków for $11 \leq N_{\mathrm{part}} \leq 17$, since the $\mathrm{d}N_{\mathrm{ch}}/\mathrm{d}\eta$ from the model matches best with the measured value in this class. DPMJET and EPOS events have been selected according to the charged particle multiplicity in the VZERO-A acceptance in order to match the experimental selection. DPMJET distributions are softer than the measured ones and the model overpredicts the production of all particles for p_{T} lower than about 0.5–0.7 GeV/c and underpredicts it at higher momenta. At high-p_{T}, the p_{T} spectra shapes of pions and kaons are rather well reproduced for momenta above 1 and 1.5 GeV/c respectively. Final state effects may be needed in order to reproduce the data. In fact, The Kraków model reproduces reasonably well the shape of pions and kaons below transverse momenta of 1 GeV/c where hydrodynamic effects are expected to dominate. For higher momenta, the observed deviations for pions and kaons could be explained in a hydrodynamic framework as due to the onset of a non-thermal component. EPOS can reproduce the pion and proton distributions within 20% over the full measured range, while larger deviations are seen for kaons and lambdas. It is interesting to notice that when final state interactions are disabled in EPOS, the description of many

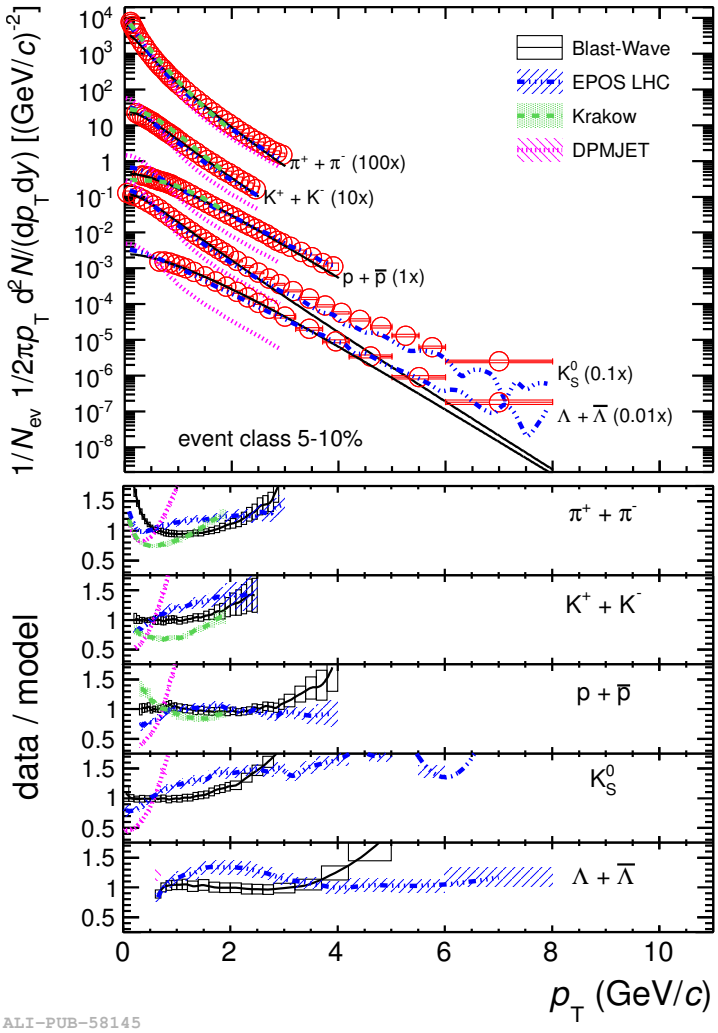

Figure 5: Pion, kaon, and proton transverse momentum distributions in the 5-10% multiplicity class compared to the several models (see text for details).

pp and p–Pb observables worsens significantly [33].

5. Conclusions

We presented a comprehensive measurement of $\pi^{\pm}$, $K^{\pm}$, K^0_S, $p(\bar{p})$ and $\Lambda(\bar{\Lambda})$ in p–Pb collisions at $\sqrt{s_{NN}}$ = 5.02 TeV at the LHC. The transverse momentum distributions show a clear evolution with multiplicity, similar to the pattern observed in high-energy pp and heavy-ion collisions, where in the latter case the effect is usually attributed to collective radial expansion. Models incorporating final state effects give a better description of the data.

References

[1] N. Cabibbo and G. Parisi, Phys. Lett. **B59**, 67 (1975).

[2] E. V. Shuryak, Phys. Lett. **B78**, 150 (1978).

[3] L. D. McLerran and B. Svetitsky, Phys. Lett. **B98**, 195 (1981).

[4] E. Laermann and O. Philipsen, Ann. Rev. Nucl. Part. Sci. **53**, 163 (2003).

[5] ALICE Collaboration, K. Aamodt *et al.*, Eur. Phys. J **C71**, 1655 (2011).

[6] ALICE Collaboration, K. Aamodt *et al.*, Eur. Phys. J. **C71**, 1594 (2011).

[7] ALICE Collaboration, B. Abelev *et al.*, Phys. Lett. **B712**, 309 (2012).

[8] ALICE Collaboration, B. Abelev *et al.*, Phys. Rev. Lett. **109**, 252301 (2012).

[9] ALICE Collaboration, B. Abelev *et al.*, (2013), hep-ex/1303.0737.

[10] CMS Collaboration, S. Chatrchyan *et al.*, Eur. Phys. J. **C72**, 2164 (2012).

[11] CMS Collaboration, V. Khachatryan *et al.*, JHEP **1105**, 064 (2011).

[12] ALICE Collaboration, B. Abelev *et al.*, Phys. Rev. Lett. **110**, 082302 (2012).

[13] ALICE Collaboration, K. Aamodt *et al.*, JINST **3**, S08002 (2008).

[14] ALICE Collaboration, B. Abelev *et al.*, Phys. Rev. Lett. **110**, 032301 (2013).

[15] J. Alme *et al.*, Nucl. Instrum. Meth. **A622**, 316 (2010).

[16] A. Akindinov *et al.*, Eur. Phys. J. Plus **128**, 44 (2013).

[17] ALICE Collaboration, Performance of the ALICE Experiment at CERN LHC, in preparation.

[18] ALICE Collaboration, (2013), nucl-ex/1307.5530.

[19] ALICE Collaboration, B. B. Abelev *et al.*, (2013), nucl-ex/1307.6796.

[20] R. Fries, B. Muller, C. Nonaka, and S. Bass, Phys. Rev. Lett. **90**, 202303 (2003).

[21] P. Bozek, (2011), nucl-th/1111.4398.

[22] B. Muller, J. Schukraft, and B. Wyslouch, Ann. Rev. Nucl. Part. Sci. **62**, 361 (2012).

[23] PHENIX Collaboration, A. Adare *et al.*, (2013), nucl-ex/1304.3410.

[24] U. W. Heinz, Concepts of heavy ion physics, CERN-2004-001-D, 2004.

[25] E. Schnedermann, J. Sollfrank, and U. W. Heinz, Phys. Rev. **C48**, 2462 (1993).

[26] E. Shuryak and I. Zahed, (2013), hep-ph/1301.4470.

[27] R. Corke and T. Sjostrand, JHEP **1103**, 032 (2011).

[28] P. Z. Skands and D. Wicke, Eur. Phys. J. **C52**, 133 (2007).

[29] H. Schulz and P. Skands, Eur. Phys. J. **C71**, 1644 (2011).

[30] A. Ortiz, P. Christiansen, E. Cuautle, I. Maldonado, and G. Paic, Phys. Rev. Lett. **111**, 042001 (2013).

[31] S. Roesler, R. Engel, and J. Ranft, p. 1033 (2000), hep-ph/0012252.

[32] P. Bozek, Phys. Rev. **C85**, 014911 (2012).

[33] T. Pierog, I. Karpenko, J. Katzy, E. Yatsenko, and K. Werner, (2013), hep-ph/1306.0121.

PoS(EPS-HEP 2013)188